In the present case of a bischelate type, however, axial association leading to generation of a paramagnetic metal center seems more likely. Stereochemistry of bis(*N*-*n*-alkylsalicylaldiminato)nickel(II) complexes was intensively studied for some time.[26] In the case of *N*-methyl derivative, for which molecular weight data over a range of concentrations indicated the association phenomenon[27] and also a fully paramagnetic isomer was isolated,[28] a polymeric (or at least dimeric in solution) structure involving axial coordination of donor oxygen atoms has been proposed. The partial paramagnetism of higher *N*-*n*-alkyl derivatives in inert solvents and in the molten state has also been reported,[29] and the pressure effect on the magnetic and spectral properties has been discussed in terms of the association equilibrium.[30] Therefore, if the substituents in the 4-position of the present *N*-*n*-propyl derivatives work in favor, such a scheme of axial coordination forming Ni-O···Ni linkages may apply to our NiL_2 complexes.

Such tendency might be extrapolated to the pure condensed phase; lathlike molecules of NiL_2 (n = 11) arranged in such a way could be regarded as a smectic-like group within the nematic domain. This kind of intermolecular interaction specific to the metal centers might affect the apparent orientational order probed by the ESR method. We would like to point out that the ^1H NMR relaxation time for NiL_2 (n = 11) in its nematic phase is roughly 0.1–0.2 s, which is shorter than that in its solid state at room temperature by an order of magnitude, although it is not certain whether this is due to a motional effect or to the paramagnetic influence. A magnetic susceptibility study of NiL_2 complexes is underway in order to clarify these points.

Experimental Section

Materials. Typical procedures for preparation of the complexes are given below.

Nickel(II) Complexes (NiL_2). 2,4-Dihydroxybenzaldehyde was subjected to DCC esterification[31] in its 4-position by an appropriate *p*-alkoxybenzoic acid,[5] and purified by several recrystallizations from methanol (or ethanol for higher homologues). A 2-mmol sample of the product was dissolved in a 70-mL quantity of hot methanol and allowed to react with 1 mmol of nickel acetate and then 2 mmol of *n*-propylamine by refluxing the mixture for 1–2 h. The resultant dark green solid was isolated by filtration, washed extensively with methanol, and purified by two or three recrystallizations from 2:1 methanol–chloroform mixtures. Yields: 70–90%, pale or dark green needlelike (n = 4–7), flaky (n = 9–12, and 14), or powdery (n = 8, 16, and 18) microcrystals. Anal. Found (calcd) for $C_{56}H_{76}N_2O_8Ni$ (n = 11): C, 69.71 (69.78); H, 8.05 (7.95); N, 2.92 (2.91). ^1H NMR ($CDCl_3$) for NiL_2 (n = 11): δ 8.94 (br s, 1 H, CH=N), 8.09 (d, J = 8.8 Hz, 2 H, benzoyl), 7.13 (d, J = 8.8 Hz, 1 H, salicylidene), 6.94 (d, 2 H, benzoyl), 6.37 (d, J = 2.2 Hz, 1 H, salicylidene), 6.31 (dd, 1 H, salicylidene), 4.03 (t, J = 6.6 Hz, 2 H, CH_2–O), 3.71 (br s, 2 H, CH_2–N), 1.91 (m, J = 7.1 Hz, 2 H, CH_2), 1.81 (m, J = 7 Hz, 2 H, CH_2), 1.52–1.27 (br m, 16 H, CH_2's), 1.01 (t, J = 7 Hz, 3 H, CH_3), 0.88 (t, J = 7 Hz, 3 H, CH_3).

Oxovanadium(IV) Complexes (VOL_2). Synthesis of VOL_2 followed an alternative route. 2-Hydroxy-4-(4-alkoxybenzoyloxy)benzaldehyde, prepared as above, was first condensed with *n*-propylamine.[10] A 2-mmol quantity of the isolated ligand was then reacted with $^1/_2$ equiv of vanadyl sulfate in methanol in the presence of triethylamine. A greenish solid formed immediately. After the mixture was refluxed for an hour, the product was collected and purified by induced crystallization from its chloroform solution by filtering, adding a saturating amount of methanol at its boiling point, and allowing it to cool down to room temperature. Yields: 40–60%, brownish gray powdery (n = 5–7, and 18), green needlelike (n = 8, 9, and 11), or flaky (n = 10, 12, 14, and 16) microcrystals with various tints. Anal. Found (calcd) for $C_{54}H_{72}N_2O_9V$ (n = 10): C, 68.86 (68.70); H, 7.71 (7.69); N, 3.02 (2.97).

Oxovanadium(IV) Complexes (C and D). The aldehyde component of the ligand in the above preparation was replaced by salicylaldehyde (for D) or its 4-benozyloxy derivative (for C) and the metalation was carried out without isolating the ligand, yielding dark green (C) and dark brown (D) microcrystals. Anal. Found (calcd) for $C_{34}H_{32}N_2O_7V$ (C): C, 64.64 (64.66); H, 5.08 (5.11); N, 4.49 (4.44). Found (calcd) for $C_{20}H_{24}N_2O_3V$ (D): C, 61.45 (61.38); H, 6.25 (6.18); N, 7.33 (7.16).

Physical Measurements. Calorimetric measurements were performed by using Rigaku Thermoflex, Rigaku TAS100, and DuPont 9900 differential scanning calorimeters. Heating or cooling rate was 5 K min^{-1}. High-resolution ^1H NMR spectra were recorded on a JEOL JNM-270 spectrometer at the Center of Instrumental Analysis, Hokkaido University. Dipolar splitting of the ^1H NMR line of neat NiL_2 (n = 11) was measured with an FT-NMR spectrometer operating at 29.8 MHz, locally constructed at Nihon University. The sample of NiL_2 (n = 11) was sealed in a 8-mm-o.d. Pyrex tube after evacuating for 30 h through a freeze–pump–thaw cycle. The X-band EPR spectra were recorded on a JEOL JES-FE1X spectrometer equipped with a high-temperature cavity controllable up to 200 °C. The samples were prepared in air by mixing a spin probe at a concentration no higher than 1 mol %.

Acknowledgment. This work was supported in part by Grants-in-Aid for Scientific Research Nos. 63740328 and 02854067 from the Ministry of Education, Science, and Culture of Japan. Support by the Japan Securities Scholarship Foundation and by the IMS Joint Studies Program (1989–1990) is also acknowledged.

(26) Holm, R. H.; O'Connor, M. J. *Progress in Inorganic Chemistry*; Wiley-Interscience: New York, 1971; Vol. 14, pp 241-401.
(27) Holm, R. H. *J. Am. Chem. Soc.* **1961**, *83*, 4683-4690.
(28) Harris, C. M.; Lenzer, S. L.; Martin, R. L. *Aust. J. Chem.* **1958**, *11*, 331-335.
(29) Sacconi, L.; Cini, R.; Ciampolini, M.; Maggio, F. *J. Am. Chem. Soc.* **1960**, *82*, 3487-3491.
(30) Ewald, A. H.; Sinn, E. *Inorg. Chem.* **1967**, *6*, 40-48.
(31) Hassner, A.; Alexanian, V. *Tetrahedron Lett.* **1978**, 4475-4478.

Notes

Contribution from the Department of Chemistry, Northwestern University, Evanston, Illinois 60208-3113

Synthesis and Structure of a New Ternary Telluride, $Cu_{1.85}Zr_2Te_6$

Patricia M. Keane and James A. Ibers*

Received December 28, 1990

Introduction

The known binary and ternary chalcogenides display unusual structural arrangements[1] and interesting physical properties.[2-4] The ternary systems of Nb and Ta involving sulfides,[5,6] selenides,[6-11] and more recently the tellurides[12-16] have been intensely

(1) Lévy, F. *Crystallography and Crystal Chemistry of Materials with Layered Structures*; Reidel Publishing Company: Dordrecht, Holland, and Boston, MA, 1976.
(2) Gamble, F. R.; DiSalvo, F. J.; Klemm, R. A.; Geballe, T. H. *Science* **1970**, *168*, 568.
(3) Delk, F. S.; Sienko, M. J. *Inorg. Chem.* **1980**, *19*, 1352-1356.
(4) Wilson, J. A. *Phys. Rev. B* **1979**, *19*, 6456-6468.
(5) Sunshine, S. A.; Ibers, J. A. *Inorg. Chem.* **1985**, *24*, 3611-3614.
(6) Meerschaut, A.; Gressier, P.; Guémas, L.; Rouxel, J. *Mater. Res. Bull.* **1981**, *16*, 1035-1040.
(7) Salem, A. B.; Meerschaut, A.; Guémas, L.; Rouxel, J. *Mater. Res. Bull.* **1982**, *17*, 1071-1079.
(8) Keszler, D. A.; Squattrito, P. J.; Brese, N. E.; Ibers, J. A.; Shang, M.; Lu, J. *Inorg. Chem.* **1985**, *24*, 3063-3067.
(9) Keszler, D. A.; Ibers, J. A. *J. Solid State Chem.* **1984**, *52*, 73-79.
(10) Keszler, D. A.; Ibers, J. A. *J. Am. Chem. Soc.* **1985**, *107*, 8119-8127.
(11) Sunshine, S. A.; Ibers, J. A. *Inorg. Chem.* **1986**, *25*, 4355-4358.
(12) Sunshine, S. A.; Keszler, D. A.; Ibers, J. A. *Acc. Chem. Res.* **1987**, *20*, 395-400.
(13) Liimatta, E. W.; Ibers, J. A. *J. Solid State Chem.* **1987**, *71*, 384-389.
(14) Liimatta, E. W.; Ibers, J. A. *J. Solid State Chem.* **1988**, *77*, 141-147.
(15) Liimatta, E. W.; Ibers, J. A. *J. Solid State Chem.* **1989**, *78*, 7-16.
(16) Mar, A.; Ibers, J. A. *J. Solid State Chem.*, in press.

0020-1669/91/1330-3096$02.50/0

Table I. Data Collection and Refinement Details for $Cu_{1.85}Zr_2Te_6$

formula	$Cu_{1.85}Zr_2Te_6$
fw	1065.60
space group	D_{2h}^{16}-*Pnma*
a, Å	10.891 (9)
b, Å	3.972 (2)
c, Å	24.00 (2)
V, Å^3	1038 (1)
Z	4
T of data collcn, K	111[a]
D(calcd), g cm^{-3}	6.82
radiation	graphite-monochromated Mo Kα (λ(Kα_1) = 0.7093 Å)
linear abs coeff, cm^{-1}	225
transm factors	0.25–0.55[b]
$R_w(F_o)$	0.038
$R(F)$ for $F_o^2 > 3\sigma(F_o^2)$	0.030

[a] The low-temperature system is based on a design by Huffman: Huffman, J. C. Ph.D. Thesis, Indiana University, 1974. [b] The analytical method was used for the absorption correction: de Meulenaer, J.; Tompa, H. *Acta Crystallogr.* **1965**, *19*, 1014–1018.

investigated. In contrast, the search for new phases of the type group IV–TM–Te, where TM = V–Zn triads, has received little attention. In fact, there are no reported phases in these ternary systems.

The ternary group IV tellurides should differ from those of Nb or Ta. Unlike Nb and Ta, which readily form MTe_2[17] and MTe_4 (M = Nb, Ta),[18] Zr and Hf are capable of forming $M'Te_2$,[19,20] $M'Te_3$,[21] and $M'Te_5$[22] (M' = Zr, Hf). The structures of $M'Te_3$,[21] $M'Se_3$,[21] and $M'S_3$[21] are similar to that of $NbSe_3$[23] so it may be possible to synthesize ternary M'–chalcogenide complexes that are related to the known ternary niobium or tantalum sulfides or selenides. However, because M' has one less d electron available than does Nb or Ta, it is more likely that compounds of M' will exhibit different structural motifs since more Te–Te bonding will be necessary to effect charge balance. Since typically the metals of the Ni triad form ternary chalcogenide compounds of Ta or Nb, a metal of the Cu triad may be necesary to maintain this general electron count in the Zr and Hf compounds.

Our initial investigation of this ternary system yields compounds with structures that are dramatically different from any of the niobium or tantalum chalcogenides. The compounds $Cu_2M'Te_3$ (M' = Zr, Hf)[24] have recently been reported, and here we describe $Cu_{1.85}Zr_2Te_6$, another new phase in the group IV–TM–Te system.

Experimental Section

A combination of the elemental powders Cu (AESAR, 99.999%), Zr (AESAR, 99%), and Te (AESAR, 99.5%) in a 4:1:6 ratio were ground together and loaded into a silica tube that was evacuated ($\sim 10^{-4}$ Torr) and sealed. The tube was heated in a furnace at 650 °C for 6 days, and then at 900 °C for 4 days. A slow cool of 3 °C/h to 450 °C and then a rapid cool of 90 °C/h to room temperature was used. The product contained crystals of two different habits. The major crystalline product consisted of shiny silver needles that formed within the melt. The exact composition of this phase was established by single-crystal X-ray studies to be Cu_2ZrTe_3.[24] The minor product $Cu_{1.85}Zr_2Te_6$ (as established from the X-ray analysis (vide infra)) grew as dull black needles at the surface of the Cu/Te melt. EDAX analysis established the presence of the three elements (Cu, Zr, Te) in both phases. A quantitative chemical analysis on the crystal selected for X-ray structure analysis was performed with the electron microprobe of an EDAX-equipped Hitachi S570 electron microscope; a Cu_2ZrTe_3 single crystal was used as a standard. The integrated intensities were corrected, and the chemical composition was derived from the computer program MICROQ.[25] All the characteristic peaks were assigned to the elements Cu, Zr, and Te; no impurities or trace elements were detected. The analysis gave the composition $Cu_{1.94}Zr_{2.00}Te_{5.91}$, in excellent agreement with that of $Cu_{1.85}Zr_2Te_6$, established in the X-ray study. Attempts to optimize the yield of this minor component have thus far failed.

Analysis of Weissenberg photographs verified the presence of two crystalline phases: Cu_2ZrTe_3[24] (monoclinic) and $Cu_{1.85}Zr_2Te_6$ (orthorhombic). For $Cu_{1.85}Zr_2Te_6$ preliminary cell constants and the space group D_{2h}^{16}-Pnma or C_{2v}^9-*Pn*2$_1$*a* were determined from overexposed films.

Final unit cell constants were determined from least-squares refinement of 23 reflections in the range $40 \le 2\theta(\text{Mo K}\alpha_1) \le 42°$ that had been automatically centered on a Picker FACS-1 diffractometer. Intensity data were collected out to $2\theta(\text{Mo K}\alpha_1) \le 65.0°$ at 111 K. Additional experimental data are given in Table I and Table IS.[26] During data collection, six standard reflections were measured every 100 reflections and exhibited no significant variations.

Calculations were performed on a Stellar GS2000 computer with programs standard in this laboratory.[27] As a satisfactory residual index (R = 0.074) was obtained from averaging the absorption corrected data in Laue group *mmm*, the centric space group was chosen. The positions of the atoms were located by direct methods.[28]

The final least-squares refinement on F_o^2 included variable site occupancy for atom Cu(2) and anisotropic thermal parameters for all atoms; 2107 unique data, including those for which $F_o^2 \le 0$, and 63 variables were involved. The resultant composition of this single crystal is $Cu_{1.845(7)}Zr_2Te_6$. While the occupancy and thermal parameters of atom Cu(2) were not highly correlated (maximum correlation coefficient < 0.50) the limits of error on the composition are probably optimistic. A

Table II. Positional Parameters and Equivalent Isotropic Thermal Parameters for $Cu_{1.85}Zr_2Te_6$

atom	*x*	*y*	*z*	B_{eq},[a] Å^2
Te(1)[b]	0.380 203 (61)	1/4	0.436 327 (28)	0.58 (1)
Te(2)	0.188 321 (59)	3/4	0.336 942 (28)	0.49 (1)
Te(3)	0.300 498 (61)	1/4	0.544 383 (29)	0.59 (1)
Te(4)	−0.000 583 (57)	1/4	0.437 279 (27)	0.48 (1)
Te(5)	0.027 346 (64)	1/4	0.195 960 (28)	0.58 (1)
Te(6)	−0.190 431 (60)	3/4	0.326 291 (29)	0.55 (1)
Zr(1)	0.191 241 (88)	3/4	0.467 666 (42)	0.50 (2)
Zr(2)	−0.005 237 (88)	1/4	0.310 954 (42)	0.50 (2)
Cu(1)	0.390 29 (12)	3/4	0.275 239 (56)	0.67 (3)
Cu(2)	0.237 14 (15)	1/4	0.253 801 (76)	1.04 (4)

[a] $B_{eq} = (8\pi^2/3)\sum_i\sum_j U_{ij}a_i^*a_j^*\mathbf{a}_i\mathbf{a}_j$. [b] All atoms are on site symmetry *m* and Wyckoff position *c*.

Table III. Selected Distances (Å) and Angles (deg) for $Cu_{1.85}Zr_2Te_6$

Zr(1)–2Te(1)	2.957 (2)	Cu(1)–Te(2)	2.652 (2)
Zr(1)–2Te(3)	2.958 (2)	Cu(1)–2Cu(2)	2.644 (2)
Zr(1)–2Te(4)	2.973 (2)	Cu(1)–2Zr(2)	3.085 (2)
Zr(1)–Te(4)	3.085 (2)	Cu(2)–Te(5)	2.673 (3)
Zr(1)–Te(2)	3.137 (3)	Cu(2)–2Te(2)	2.865 (2)
Zr(2)–Te(5)	2.782 (3)	Cu(2)–2Te(6)	2.874 (2)
Zr(2)–2Te(6)	2.854 (2)	Cu(2)–Cu(1)	2.644 (2)
Zr(2)–2Te(2)	2.963 (2)	Cu(2)–Zr(2)	2.975 (3)
Zr(2)–Te(4)	3.032 (3)	Cu(2)–Zr(2)	3.207 (3)
Zr(2)–Cu(2)	2.975 (3)	Te(1)–Te(3)	2.735 (2)
Zr(2)–2Cu(1)	3.085 (2)	Te(1)–2Te(3)	4.031 (3)
Cu(1)–2Te(5)	2.579 (2)	Te(1)–2Te(1)	3.972 (3)
Cu(1)–Te(6)	2.590 (2)	Te(3)–2Te(3)	3.972 (3)
Te(1)–Zr(1)–Te(4)	88.74 (5)	Te(6)–Zr(2)–Te(5)	102.59 (3)
Te(1)–Zr(1)–Te(3)	55.07 (4)	Te(2)–Cu(1)–Te(5)	109.30 (5)
Te(3)–Zr(1)–Te(4)	89.25 (5)	Te(2)–Cu(1)–Te(6)	104.11 (7)
Te(2)–Zr(1)–Te(4)	137.11 (5)	Te(5)–Cu(1)–Te(6)	116.65 (4)
Te(1)–Zr(1)–Te(1)	84.37 (6)	Te(5)–Cu(1)–Te(5)	100.73 (7)
Te(4)–Zr(2)–Te(2)	77.15 (3)	Te(5)–Cu(2)–Te(2)	101.72 (6)
Te(4)–Zr(2)–Te(6)	83.27 (3)	Te(5)–Cu(2)–Te(6)	83.53 (6)
Te(4)–Zr(2)–Te(5)	171.71 (4)	Te(6)–Cu(2)–Te(6)	92.16 (6)
Te(2)–Zr(2)–Te(5)	96.78 (3)	Te(2)–Cu(2)–Te(2)	87.76 (6)
		Te(6)–Cu(2)–Te(2)	92.16 (6)

(17) Brown, B. E. *Acta Crystallogr.* **1966**, *20*, 264–267.
(18) Bronsema, K. D.; van Smaalen, S.; de Boer, J. L.; Wiegers, G. A.; Jellinek, F. *Acta Crystallogr.* **1987**, *B43*, 305–313.
(19) Bear, J.; McTaggart, F. K. *Aust. J. Chem.* **1958**, *11*, 445–470.
(20) Brattås, L.; Kjekshus, A. *Acta Chem. Scand.* **1971**, *25*, 2783–2785.
(21) Furuseth, S.; Brattås, L.; Kjekshus, A. *Acta Chem. Scand.* **1975**, *A29*, 623–631.
(22) Furuseth, S.; Brattås, L.; Kjekshus, A. *Acta Chem. Scand.* **1973**, *27*, 2367–2374.
(23) Meerschaut, A.; Rouxel, J. *J. Less-Common Met.* **1975**, *39*, 197–203.
(24) Keane, P. M.; Ibers, J. A. *J. Solid State Chem.*, in press.
(25) *MICROQ Version 3L*; Tracor Northern Co.: Middleton, WI, 1987.
(26) Supplementary material.
(27) Waters, J. M.; Ibers, J. A. *Inorg. Chem.* **1977**, *16*, 3273–3277.
(28) Sheldrick, G. M. *Crystallographic Computing 3*; Sheldrick, G. M.; Kruger, C.; Goddard, R., Eds.: Oxford University Press: London, New York, 1985; pp 175–189.

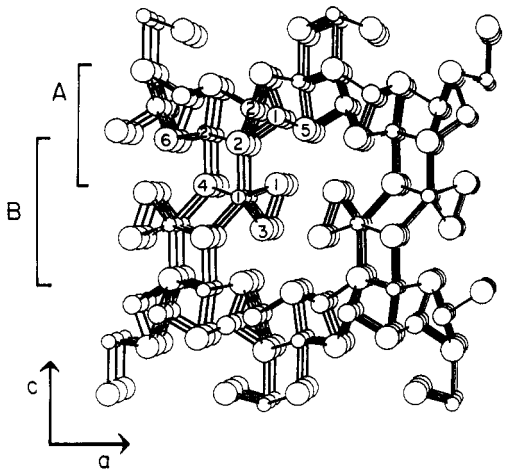

Figure 1. View of $Cu_{1.85}Zr_2Te_6$, down [010] with atoms and subunits labeled. Zr atoms are small circles, Cu atoms are medium circles, Te atoms are large circles.

final difference electron density map shows no peaks greater than 2.8% the height of a Cu atom. Analysis of $\sum w(F_o^2 - F_c^2)^2$ as a function of Miller indices, F_o^2, and setting angles exhibits no unusual trends. Final values of the atomic parameters are given in Table II. Anisotropic thermal parameters are given in Table IIS while structure amplitudes are given in Table IIIS.[26]

Results and Discussion

Important bond angles and distances are provided in Table III. Figure 1 provides a view of the structure with the labeling scheme. $Cu_{1.85}Zr_2Te_6$ displays a remarkable variety of metal coordination geometries (i.e. bicapped trigonal prisms, octahedra, square pyramids, and tetrahedra) as well as numerous types of polyhedra connectivity.

This compound contains two crystallographically distinct Zr atoms. The Zr(1) atom is at the center of a bicapped-trigonal prism of Te atoms, which exhibits a Te–Te single bond of length 2.735 (2) Å along the edge of the trigonal prism. This Te–Te distance is similar to those found in other tellurides that exhibit bicapped trigonal prismatic coordination, such as $HfTe_5$[22] (2.763 (4) Å), $ZrTe_3$[21] (2.761 (3) Å), and $K_4Hf_3Te_{17}$[29] (2.804 (5)–2.933 (4) Å). The Zr(1)–Te distances of the slightly distorted trigonal prism range from 2.957 (2) to 2.973 (2) Å. The Zr(1)–Te distances of the capping Te atoms (3.085 (2) and 3.137 (3) Å) are slightly longer than in the previously mentioned compounds (2.960 (2) Å in $HfTe_5$[22] and 3.030 (4) Å in $ZrTe_3$[21]). The Zr(2) atom is in distorted octahedral coordination with Te atoms, with Zr(2)–Te distances from 2.782 (2) to 3.032 (3) Å and Te–Zr(2)–Te bond angles from 75.68 (3) to 109.22 (6)°.

Similarly, there are two crystallographically distinct Cu atoms. The Cu(1) atom is at the center of a distorted tetrahedron of Te atoms with distances ranging from 2.579 (2) to 2.652 (2) Å. The Cu(2) atom is much more loosely held in distorted-square-pyramidal coordination with equatorial Cu(2)–Te distances ranging from 2.865 (2) to 2.874 (2) Å and the axial distance of 2.673 (2) Å. The Cu(2) atom lies approximately 0.39 Å above the basal plane. The relatively high value of B_{eq} for the Cu(2) atom (Table II) arises mainly from the root-mean-square thermal displacement in the [001] direction, which is approximately twice that of any of the other atoms. We assume this increased thermal motion arises primarily from the looser coordination about the Cu(2) atom, especially in the basal plane of its square pyramid.

The complex framework of $Cu_{1.85}Zr_2Te_6$ can be described in terms of the connectivity of these coordination polyhedra, which exhibit vertex, edge, and face sharing in all three crystallographic directions. These results are summarized in Table IV.

The metal atoms in this structure are closely interacting. The Zr(2) atom is bonded to both the Cu(1) and the Cu(2) atoms at 3.085 (2) and 2.975 (3) Å; the Cu(1) atom to the Cu(2) atom

Table IV. Three Dimensional Polyhedral Connectivity in $Cu_{1.85}Zr_2Te_6$[a]

[100]	[010]	[001]
face sp_y/oct	edge oct/oct	face bctp/oct
edge sp_y/tet	edge sp_y/sp_y	edge bctp/spy_y
edge oct/tet	vertex tet/tet	vertex bctp/tet
face bctp/bctp	face bctp/bctp	

[a] Key: sp_y = square pyramid; bctp = bicapped trigonal prism; oct = octahedron; tet = tetrahedron.

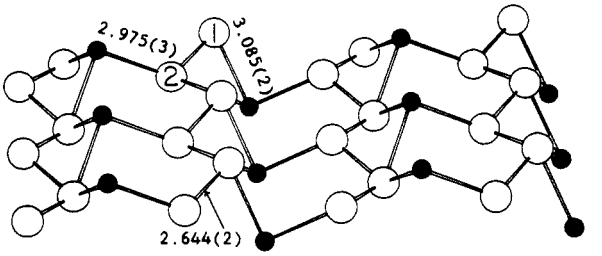

Figure 2. Drawing of a layer of metal atoms in $Cu_{1.85}Zr_2Te_6$ orthogonal to [001] at $z = {}^1/_4$ and ${}^3/_4$ with Cu–Cu and Cu–Zr interactions and distances shown. Medium filled circles are Zr atoms; large open atoms are Cu atoms.

at a distance of 2.644 (2) Å. As the distances in elemental hexagonally closest packed Zr and Cu are 3.234[30] and 2.556 Å,[31] respectively, the above distances clearly represent bonding interactions. These three metal–metal bonds interconnect to create a two dimensional array of interfused four- and six-membered rings. These buckled layers extend orthogonal to [001] at approximately $z = {}^1/_4$ and ${}^3/_4$. The four- and six-membered rings are comprised of (two Cu(1), one Cu(2), and one Zr(2) atoms) and (two Zr(2), two Cu(2), and two Cu(1) atoms), respectively. Similar layers of metal–metal bound atoms are found in Cu_2HfTe_3,[24] which is isostructural with the primary phase of this reaction, Cu_2ZrTe_3. These arsenic-like layers extend along (2̄01) between the hexagonally closest packed layers of Te atoms. This layer is illustrated in Figure 2.

The $Cu_{1.85}Zr_2Te_6$ structure contains one short single-bond interaction (Te(1)–Te(3)) among the six crystallographic distinct Te atoms. The remaining Te···Te interactions are between 3.327 (2) Å and the Te^{2-}···Te^{2-} distance of 4.2 Å.[32] The mutual interactions between the (Te(1)–Te(3)) pairs are weak, as clearly demonstrated by the long Te···Te contacts (Te(1)···Te(1) and Te(3)···Te(3) of 3.972 (3) Å and Te(1)···Te(3) of 4.031 (3) Å), which are slightly shorter than the corresponding van der Waals distance of 4.2 Å.

The physical properties of $Cu_{1.85}Zr_2Te_6$ should be interesting. However, insufficient sample is available for magnetic measurements and single crystals of length suitable for resistivity measurements have not yet been grown. $ZrTe_3$, which is structurally related to layer B, contains these capping and apical Te atoms shared between Zr-centered bicapped trigonal prisms. As $ZrTe_3$ is metallic,[33] we expect that these Zr-centered dimers will contribute to a metallic behavior of $Cu_{1.85}Zr_2Te_6$.

Acknowledgment. This research was supported by the U.S. National Science Foundation Grant DMR88-13623. The SEM facilities of the Materials Research Center at Northwestern University were used. (U.S. National Science Foundation Grant DMR88-21571).

Supplementary Material Available: Crystallographic and refinement details (Table IS) and anisotropic thermal parameters (Table IIS) (3 pages); observed and calculated structure amplitudes for $Cu_{1.85}Zr_2Te_6$ (Table IIIS) (9 pages). Ordering information is given on any current masthead page.

(29) Keane, P. M.; Ibers, J. A. *Inorg. Chem.* **1991**, *30*, 1327–1329.
(30) Evans, D. S.; Raynor, G. V. *J. Nucl. Mater.* **1961**, *4*, 66–69.
(31) Krull, W. E.; Newman, R. W. *J. Appl. Crystallogr.* **1970**, *3*, 519–521.
(32) Shannon, R. D. *Acta Crystallogr.* **1976**, *5*, 134.
(33) McTaggart, F. K. *Aust. J. Chem.* **1958**, *11*, 471–480.